Bonding configuration and density of defects of SiO x H y thin films deposited by the electron cyclotron resonance plasma method

E. San Andrés, A. del Prado, I. Mártil, G. González-Daz, D. Bravo, F. J. López, M. Fernández, W. Bohne, J. Röhrich, B. Selle, and I. Sieber

Citation: Journal of Applied Physics **94**, 7462 (2003); doi: 10.1063/1.1626798
View online: http://dx.doi.org/10.1063/1.1626798
View Table of Contents: http://scitation.aip.org/content/aip/journal/jap/94/12?ver=pdfcov
Published by the AIP Publishing

Bonding configuration and density of defects of SiO_xH_y thin films deposited by the electron cyclotron resonance plasma method

E. San Andrés, A. del Prado, I. Mártil,[a] and G. González-Díaz
Departamento de Física Aplicada III, Facultad Ciencias Físicas, Universidad Complutense, E-28040 Madrid, Spain

D. Bravo and F. J. López
Departamento de Física de Materiales, Facultad de Ciencias, C IV, Universidad Autónoma de Madrid, E-28049 Madrid, Spain

M. Fernández
Instituto de Ciencia de los Materiales, C. S. I. C., E-28049 Cantoblanco, Spain

W. Bohne, J. Röhrich, B. Selle, and I. Sieber
Hahn-Meitner-Institut Berlin, Glienicker Strasse 100, D-14109 Berlin, Germany

(Received 14 May 2003; accepted 22 September 2003)

The composition, bonding configuration, hydrogen content, and paramagnetic defects of SiO_xH_y thin films were studied. Films were deposited by the electron cyclotron resonance plasma method at room temperature using SiH_4 and O_2 as precursor gases. The film composition was measured by heavy ion elastic recoil detection analysis and energy dispersive x-ray spectroscopy. Suboxide films with compositions ranging from SiO_2 to $SiH_{0.38}$ were obtained. Infrared spectroscopy showed the presence of different Si–O and Si–H vibration modes. The usual estimation of the oxygen to silicon ratio by the wave number of the Si–O–Si stretching band was not accurate for films far from stoichiometry. These off-stoichiometric films also showed a broader Si–O–Si stretching peak than the stoichiometric ones, indicating a higher bonding disorder. The position of the Si–O–Si bending and rocking modes did not depend on the film composition. On the other hand, the peak position of the Si–H modes were found strongly dependent on the Si environment. By single-wavelength ellipsometry at $\lambda = 632.8$ nm the refractive index n was found to range between 1.45 (SiO_2) and 2.04 ($SiO_{0.06}H_{0.36}$). Electron spin resonance measurements showed that stoichiometric films presented the well known E' center ($\cdot Si \equiv O_3$) with concentrations in the 10^{16}–10^{17} cm^{-3} range, while for Si-rich films ($x \ll 1$) the Si dangling bond center (Si_{DB}, $\cdot Si \equiv Si_3$) was the only detectable defect, with concentrations in the 10^{18}–10^{19} cm^{-3} range. In near-stoichiometric films both E' and Si_{DB} centers were found. © *2003 American Institute of Physics.* [DOI: 10.1063/1.1626798]

I. INTRODUCTION

Si-rich SiO_x films (SROX) have a wide and increasing interest in the field of Si-based device technology due to several reasons:

(i) SROX layers are always present at the Si/SiO_2 interface[1] even on thermally grown SiO_2[2] and also on many high-K dielectric/Si interfaces.[3] The presence of these suboxide layers and their characteristics are strongly dependent on surface preparation, deposition process, annealing parameters, etc. These suboxides may generate interface defect states which limit the dielectric performance when used in MOS structures.[1]

(ii) Recently SROX films have found application in nonvolatile memory devices, where the use of a stack of dielectrics $SROX/SiO_2$ reduces the erasing time and the threshold voltage.[4–6]

(iii) Annealed SROX films show the presence of Si nanocrystals (nc-Si).[7] Much work is being done on the electroluminescence properties of these nc-Si embedded in a SiO_2 matrix.[8,9] This is an interesting issue due to its potential optoelectronic applications.

(iv) By now, to increase the electrical performance of MOSFET devices there is a constant reduction in gate lengths. Therefore, higher values of the capacitance per unit area of the gate dielectric [$C_{diel} = (\varepsilon)/t_{diel}$, where ε is the dielectric permittivity and t_{diel} is the dielectric thickness] are necessary. With thermally grown silicon dioxide (SiO_2) as gate insulator a gate oxide thickness of 2–3 nm will be needed. The problem of using such a thin SiO_2 film is the occurrence of high gate leakage currents. SROX films, with a higher permittivity value, between 3.8 (SiO_2)[10] and 11.9 (Si),[11] allow gates thicker than those made of SiO_2 with the same capacitance per unit area. But the problem with SROX is its decreasing band gap when the Si content increases, so the advantage in permittivity may be lost by gate leakages.

Some physical characteristics of SROX films that influence device performance and reliability are, among others, the high hydrogen content and the presence of paramagnetically active defects (e.g., dangling bonds).[12] The hydrogen is bonded in different configurations ($Si{=}H_2$, $Si_nO_{3-n} \equiv Si{-}H$, etc.)[13] depending on the film deposition process and

[a]Author to whom correspondence should be addressed; electronic mail: imartil@fis.ucm.es

on the suboxide composition. The bonded hydrogen and its configuration can be detected by Fourier transform infrared spectroscopy (FTIR).[14] The dangling bonds (usually paramagnetic) play a key role in the device performance.[15] Depending on the film composition, the dominant defect has a different microscopic structure, changing its type from the well known E' center ($\cdot Si \equiv O_3$) in stoichiometric SiO_2 films to the Si-dangling bond defect ($\cdot Si \equiv Si_3$, in the following Si_{DB}) in SROX films far from the stoichiometry.[16] The study of defects in SROX films is scarce and few articles dealing with this problem can be found in the literature.[12,17]

There are many different techniques to grow SROX films.[12,18–20] A desirable objective is a low thermal budget in the growing process. Not all deposition processes fulfill this requirement. Low thermal budget is desirable because if the gate growth process takes place at high temperatures, the preceding processes (mainly the implantations) may suffer from degradation, resulting in nonfunctional devices. Plasma processes are able to deposit thin dielectric films at low temperatures in short times, so much effort has been made to get films with device characteristics from plasma-excited gases.[13,21–23] This plasma can be generated by different procedures; among them the electron cyclotron resonance plasma method (in the following ECR) shows various advantages:

(i) It is a remote plasma system due to the separation between the plasma generation zone and the deposition chamber. Then, only neutral atoms and radicals are able to reach the substrate surface. As a consequence any damage which could be generated by ion bombardment or plasma irradiation is significantly reduced.[24]

(ii) The degree of activation of species is significantly superior in ECR plasmas than in other plasma methods.[25]

(iii) With the ECR plasma method, high quality gate dielectrics can be deposited at low deposition temperatures,[26] achieving the objective of the low thermal budget.

The aim of this article is to analyze the bonding structure of SROX films and the type and concentration of paramagnetic defects present as a function of the actual film composition. The analyzed films were deposited at room temperature by the ECR method. The deposition parameters were adjusted to scan the range of compositions from stoichiometric SiO_2 to SiH_y.

II. EXPERIMENT

Several series of films were deposited onto a simplified Radio Corporation of America (RCA) cleaned high-resistivity (80 Ω cm) Si(111) substrates polished on both sides. The substrates had dimensions of 1×1 cm^2. The deposition processes were carried out at a base pressure of 6×10^{-7} mbar in a homemade chamber attached to an Astex 4500 ECR reactor. Further details about the deposition system are given elsewhere.[27] High purity SiH_4 and O_2 were used as precursor gases. Films of several compositions were obtained depending on the gas flow ratio, that we define in this article in the same way as Bulkin *et al.*,[18] i.e., as $\mathbf{R_b}=[SiH_4]/([SiH_4]+[O_2])$. In this study, $\mathbf{R_b}$. was varied between 0.2 and 1. For all depositions, the total gas flow, the total pressure and the microwave power were kept constant at 10.5 sccm, 9.3×10^{-4} mbar, and 100 W, respectively. The substrates were not intentionally heated and the deposition temperature was in the 50–60 °C range. The thickness of the deposited films was about 250 nm, measured with a Dektak profilometer. Low values of $\mathbf{R_b}$ (below 0.4) resulted in stoichiometric, almost hydrogen-free SiO_2 films, while higher values (in the 0.6–0.9 range) yielded off-stoichiometric films with high hydrogen content. These films will be referred as SiO_xH_y (with x the oxygen to silicon ratio of the films and y the hydrogen to silicon ratio). At $\mathbf{R_b}=1$ no O_2 was introduced into the deposition chamber. These films did not exhibit oxygen incorporation and will be referred to as SiH_y.

The composition, the bonding configuration, the concentration of paramagnetic defects as well as the refractive index of films were obtained by means of heavy ion elastic recoil detection analysis (HI-ERDA) and energy dispersive x-ray spectroscopy (EDX), Fourier transform infrared spectroscopy (FTIR), electron spin resonance (ESR), and ellipsometric measurements, respectively.

The HI-ERDA measurements were carried out with a mass and energy dispersive time-of-flight (ToF) setup.[28] The ions used as projectiles were 230 MeV ^{129}Xe ions provided by the ion beam facility (ISL) of the Hahn-Meitner-Institut in Berlin. The detection system with a solid angle of 0.4 msr and the use of a large detection angle of 60° provided reasonable measuring statistics, even at ion fluences as low as 10^{12} ions cm^{-2}. The number of incident particles was measured with an accuracy of 2% using a ''transmission Faraday cup.''[29] Some samples showed hydrogen loss during the measuring process. To obtain the zero dose hydrogen concentration, an effusion model, previously described,[30] was used. These measurements provided the absolute composition of the samples, i.e., the x and y values of the SiO_xH_y formula, without the need of calibration samples.

EDX measurements were performed with a Hitachi S-4100 scanning microscope attached to a Si-Q-Detector Pioneer of NORAN. The acceleration voltage was 5 keV and the takeoff angle was 30°. The correction was calculated by the Proza method.[31] A certified SiO_2 stoichiometric layer deposited by LPCVD was used as a calibration standard. Since EDX was not able to detect hydrogen, these measurements provided only information on the x value. The x values obtained by EDX were very similar to those obtained by HI-ERDA. In the following the averaged value of x measured by EDX and measured by HI-ERDA will be used as the actual oxygen to silicon ratio of the films.

FTIR characterizations were done in the 400–4000 cm^{-1} range with a Nicolet Magna-IR 750 series II spectrometer working in the transmission mode at normal incidence. The spectrum of the film was obtained by subtracting the spectrum of a bare-Si sample from the total signal (substrate+deposited film). Additionally, the baselines of the resulting spectra were corrected and, thus, the main characteristics were measured. Following articles of the North Carolina State University group,[13,32] the peak position of the main Si–O–Si stretching band can be used to measure the oxygen to silicon ratio of the films. We will compare

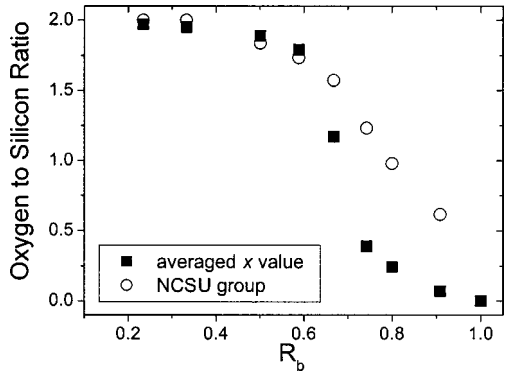

FIG. 1. Oxygen to silicon ratio (x) of the films as a function of the gas flow ratio R_b : averaged x values from HI-ERDA and EDX (■), estimate by the equation $x=0.020\ \nu_{st}-19.3$ of the NCSU group (see Refs. 14 and 33) (○).

these results with the actual x value obtained by HI-ERDA and by EDX.

ESR characterization was performed at room temperature with a Bruker ESP 300E spectrometer operating in the X band at a microwave power of 0.5 mW. This signal level is low enough to prevent the saturation of the signal. In order to enhance the ESR signal each film used was cut into five pieces of 0.2×1 cm. These five pieces were stacked, so the effective thickness of each sample was about 1250 nm. The density of paramagnetic centers was quantified by comparison with the signal of a calibrated weak pitch standard.[26]

Thinner samples (80 nm thick) were characterized by ellipsometry to obtain the refractive index n of the SiO_xH_y films. These measurements were performed with a Gaertner L116B ellipsometer operated at $\lambda=632.8$ nm.

III. RESULTS

A. Structural characterization

Figure 1 shows the oxygen to silicon ratio (x) of the SiO_xH_y films, as obtained from HI-ERDA and EDX measurements. This value ranges from $x=1.97$ for the samples deposited with $\mathbf{R_b}$ ratios below 0.4 to $x=0$ for the sample deposited at $\mathbf{R_b}=1$. This way, samples of the entire range from stoichiometric SiO_2 to SiH_y were obtained by our deposition method.

In Fig. 2, the FTIR spectra in the 400–1450 and 1800–2300 cm^{-1} ranges are displayed for some selected samples with representative compositions. No vibrational features were found in the other parts of the spectra. The most intense feature in the spectra appeared around 1068–1000 cm^{-1} with a shoulder at 1120 cm^{-1}. This is the well known Si–O–Si stretching vibration, from which the North Carolina State University physics group[14,33] (in the following, NCSU group) obtained the empirical law:

$$x=0.020\ \nu_{st}-19.3, \tag{1}$$

where ν_{st} is the wave number of the Si–O–Si peak and x is the oxygen to silicon ratio of the SiO_xH_y. For comparison, the x values estimated from Eq. (1) are also included in Fig. 1. It can be seen that the data of both methods agree well for compositions above 1.5, whereas the x value for silicon rich SiO_xH_y films is largely overestimated by Eq. (1). The reason

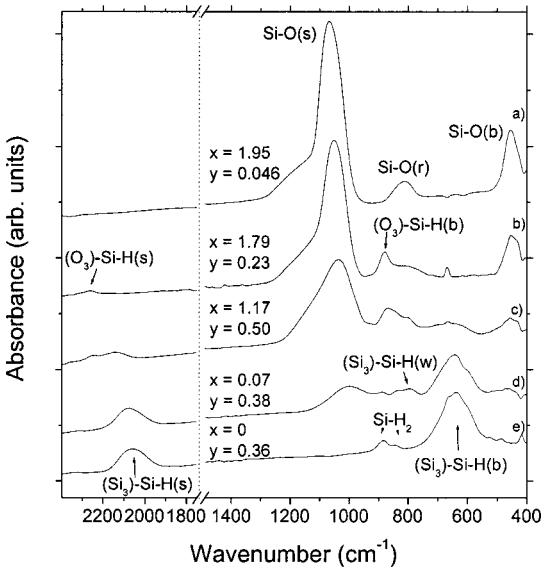

FIG. 2. FTIR absorbance spectra of five representative SiO_xH_y samples in the 400–1450 and 1800–2300 cm^{-1} ranges: (s) stretching, (b) bending, (r) rocking.

for this discrepancy is probably the higher hydrogen content of our samples as compared to those studied by the NCSU group.[13,32] This fact will be the subject of a forthcoming article.

In Fig. 3 the full width at half maximum (FWHM) of the Si–O–Si stretching peak is plotted as a function of x. This parameter gives an indication of the film quality, due to its relation with bonding disorder, porosity, stress, etc.[16,33–35] Thermally grown SiO_2 presents a value of this parameter around 75 cm^{-1}.[36]

Figures 1, 2, and 3 show these results:

(i)$\mathbf{R_b<0.35:}$ For these samples, x ranged between 1.97 and 1.95 and y between 0.034 and 0.046. As an example of this type of films Fig. 2(a) shows the spectrum of a film deposited with $\mathbf{R_b}=0.33$. In this spectrum only Si–O related vibrational modes were observed. The main vibration is located at 1068 cm^{-1} with a shoulder at 1121 cm^{-1} and a FWHM of 87 cm^{-1}. This known feature is the Si–O–Si stretching mode of a stoichiometric SiO_2 film.[37] The other two detected peaks correspond to the Si–O–Si bending and

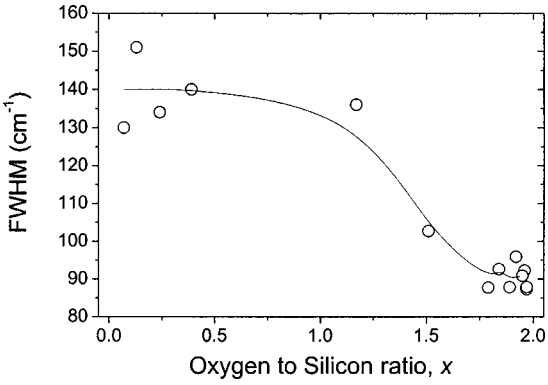

FIG. 3. FWHM of the Si–O–Si stretching band as a function of x for all the SiO_xH_y samples analyzed. The line is a guide to the eye.

rocking vibrations, located at 815 and 455 cm^{-1}, respectively. The FTIR spectra of these samples have the same characteristics as the spectrum of a high quality SiO_2 film.[1] The HI-ERDA results showed that there was a small amount of hydrogen (about 1.2 at. %). This hydrogen could not be observed in the FTIR spectra due to the detection limit of this technique ($\sim 2\%$). If it is assumed that each Si, O, and H atom has 4, 2, and 1 unpaired valence electrons, respectively, then the number of electrons of each species that can form a bond can be found. H atoms are only bonded to Si, since no O–H modes were found. The remaining concentration of nonsaturated Si electrons is the same as the concentration of unpaired O electrons. This way it is deduced that only Si–H and Si–O bonds are present, and no Si–Si bonds. Thus, the film can be considered as stoichiometric SiO_2 with a small H incorporation. In the following these films will be referred to as stoichiometric samples.

(ii) $\mathbf{0.35 < R_b < 0.6:}$ For these samples x ranged between 1.89 and 1.79 and y between 0.25 and 0.23. As an example, Fig. 2(b) shows the spectrum of a sample deposited at $\mathbf{R_b} = 0.59$. The Si–O–Si related vibrations were present, but their characteristics differed from those of stoichiometric SiO_2: while the FWHM of the stretching vibration was around 90 cm^{-1} (indicating a low bonding disorder[38]) the wave number of the Si–O–Si stretching peak shifted from 1064 to 1045 cm^{-1} when $\mathbf{R_b}$ varied from 0.35 to 0.60. The Si–O–Si rocking and bending peaks appeared at the same wave number as for a SiO_2 sample. In these films two additional peaks were detected: a small feature at 2269 cm^{-1} and a more intense one at 880 cm^{-1}. These two peaks are related to bonded H, and will be discussed later on. Previous results obtained for rapid-thermally annealed SiO_xH_y films[33] showed that there was a significant amount of nonbonded H incorporated in these films. Once more, it is deduced that H atoms are only bonded to Si, since no O–H modes were found. HI-ERDA showed that there were more remaining Si electrons (nonbonded to H) than O valence electrons, so it can be concluded that Si–Si bonding and Si dangling bonds are more favorable. The films deposited within this range of $\mathbf{R_b}$ will be referred to as near-stoichiometric samples.

(iii) $\mathbf{0.6 < R_b < 1:}$ For these samples, x ranged from 1.17 ($\mathbf{R_b} = 0.65$) to 0.07 ($\mathbf{R_b} = 0.9$). At the same time y changed from 0.50 to 0.38. Two spectra of these samples are shown in Figs. 2(c)–2(d). The wave number of the Si–O–Si stretching peak shifted from 1045 cm^{-1} to 1013 cm^{-1}. The intensity of all Si–O–Si related peaks decreased when x decreased. The rocking as well as the bending modes vanished for x values below 1.1. Figure 3 shows that in this range of $\mathbf{R_b}$ the FWHM of the Si–O–Si stretching peak increased from 90 cm^{-1} (near-stoichiometric value) to about 140 cm^{-1} ($x < 1.3$). This result indicated that the increasing Si and H content of the films promoted a significant increase in bonding disorder.[39] There were also two hydrogen related peaks: a feature at around 2100 cm^{-1}, and a more intense one at 640 cm^{-1}, which will be discussed later on. In the following these films will be called off-stoichiometric SiO_xH_y.

(iv) $\mathbf{R_b = 1:}$ In this sample no oxygen was detected and its y value is 0.36. The FTIR spectrum features of this sample is shown in Fig. 2(e). As expected, this film did not show any Si–O–Si related peaks and only Si–H peaks were found. In the following this film will be named $SiH_{0.36}$.

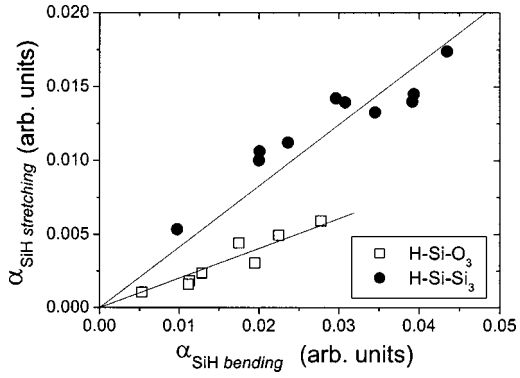

FIG. 4. Comparison of the absorption coefficients at 880 and 2260 cm^{-1} (□) and at 640 and 2100 cm^{-1} (●). Solid lines: linear fits of the data.

In the next paragraphs the Si–H bonding results will be outlined in some more detail. Near-stoichiometric samples showed a peak around 2260 cm^{-1}. This is the well known Si–H stretching vibration of the $H–Si{\equiv}O_3$ configuration. The spectra of these samples also exhibited a peak at 880 cm^{-1} which is not as well documented. The NCSU group[13] proposed that this peak corresponds to the bending vibration of the $H–Si{\equiv}O_3$ group. Our results support this assignment by two facts: both peaks appear in the same samples, and a strong correlation between the absorption coefficient of both modes is observed. Figure 4 displays the absorption coefficient of the peak at 2260 cm^{-1} versus the absorption coefficient of the peak at 880 cm^{-1} (open squares). The linear fit (through zero) of these data gives a proportionality factor $(\alpha_{2260})/(\alpha_{880}) = 0.20 \pm 0.03$, which is in good agreement with the findings of the NCSU group.[13] Thus, our results further confirmed the fact that the 2260 and 880 cm^{-1} peaks are related to bonded hydrogen in the $H–Si{\equiv}O_3$ configuration.

As the Si content increased, the peak at 2260 cm^{-1} showed a more complex structure. When x decreased below 1.9 a shoulder in the 2060–2200 cm^{-1} region appeared. This shoulder is a first neighbors effect: when the Si atom of a Si–H bond is not only bonded to oxygen but also to other Si atoms, the wave number of the Si–H stretching vibration changes. If the Si–H group is written as $H–Si{\equiv}(O_nSi_{3-n})$, then each of these groups presents vibrations at 2000, 2100, 2195, and 2250 cm^{-1} for $n = 0$, 1, 2, and 3, respectively.[39] They are strongly dependent on the chemical environment of the bond,[1] so significant shifts from these reported positions are expected for SiO_xH_y films with intermediate compositions.

Owing to the complex shape of the 2260 cm^{-1} Si–H peak when the shoulder was present it was difficult to measure the exact wave number of the intermediate modes: $H–Si{\equiv}(OSi_2)$ and $H–Si{\equiv}(OSi_2)$. Our results gave values of 2200 and 2150 cm^{-1} for these modes, respectively. These wave numbers may be affected by a significant uncertainty, due to the very weak absorption of the intermediate modes. In spite of this, they were in good agreement with the ones

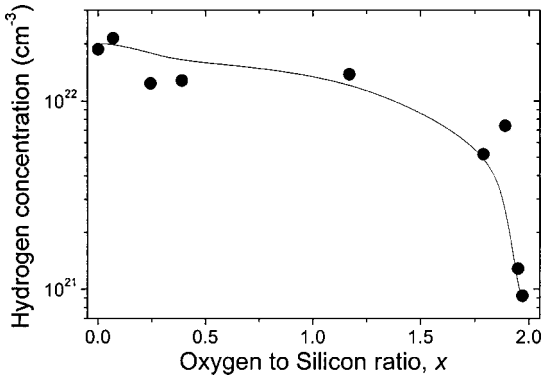

FIG. 5. Hydrogen content as a function of x for SiO_xH_y films determined by HI-ERDA. The line is a guide to the eye.

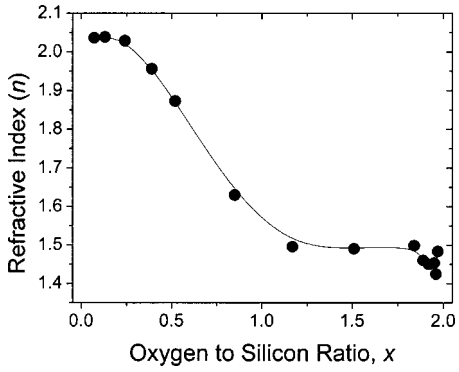

FIG. 6. Refractive index (n) at $\lambda = 632.8$ nm as a function of x for SiO_xH_y films. The line is a guide to the eye.

calculated by the NCSU group[1] for intermediate SiO_xH_y compositions.

The other peak observed in the high wave number region was a mode at 2150–2050 cm^{-1} (see Fig. 2). It corresponds to the $H–Si{\equiv}Si_3$ stretching vibration in a suboxide environment. This peak became detectable for x values below 1.6. With increasing Si content this peak became more intense, even masking the contributions of other intermediate modes. For the samples with this peak a further intense vibration at 640 cm^{-1} was also detected (see Fig. 2). This vibration is known as the bending vibration of the $H–Si{\equiv}Si_3$ bond.[40] In Fig. 4 the absorption coefficient of the peak at 2100 cm^{-1} as a function of the absorption coefficient of the peak at 640 cm^{-1} (solid circles) is also shown. The linear fit through zero of these data gives a proportionality factor $(\alpha_{2100})/(\alpha_{640}) = 0.41 \pm 0.04$. Since there is a strong correlation between the absorption coefficient of the 2100 and 640 cm^{-1} peaks, these results also confirm that both peaks are related to bonded hydrogen in the same configuration, i.e., to the $H–Si{\equiv}Si_3$ group.

In the case of off-stoichiometric films three additional peaks of low intensity were detected at 795, 840, and 885 cm^{-1} (see Fig. 2). Owing to their proximity in wave number these peaks were hardly resolved. The peak located at 795 cm^{-1} can be associated to a coupled mode between Si–H bonds in the same plane as a Si–O–Si bond.[41] The couple of peaks at 840 and 885 cm^{-1} is a doublet (wagging-bending) for $(Si{=}H_2)_n$ groups.[14] The presence of this doublet indicates that there is a small amount of hydrogen bonded in the form of a dihydride.

Finally, as presented before, the $SiH_{0.36}$ film did not show any Si–O related peaks, and only Si–H modes were detected [Fig. 2(e)]: the expected $H–Si{\equiv}Si_3$ bending vibration at 640 cm^{-1}, the $H–Si{\equiv}Si_3$ stretching vibration at 2060 cm^{-1}, and two faint peaks at 840 and 885 cm^{-1} which are related to silicon dihydride. In this sample the peak at 795 cm^{-1} did not appear.

Figure 5 shows the total hydrogen concentration of the films, measured by HI-ERDA, as a function of the oxygen to silicon ratio. It can be seen that near-stoichiometric and off-stoichiometric samples contain a very high amount of bonded hydrogen (20–27 at. %).

The refractive index n as a function of x is shown in Fig. 6. It can be seen that for samples with x above 1.2 the n value was 1.46 ± 0.03 in all cases, i.e., an n value comparable to the one of thermally grown SiO_2.[42] As x changes from $x = 1.2$ to $x = 0$ the refractive index increased from $n = 1.46$ to $n = 2.04$. These results are consistent with the work of Lin *et al.*[12] who showed that the increase of the refractive index for SiO_xH_y films is a direct consequence of the growing silicon content in the film.

B. Content of paramagnetic defects

The ESR derivative spectra of some representative samples are presented in Fig. 7. In these spectra several types of paramagnetic defects can be observed:

(i) A narrow line with g ranging from 2.0004 to 2.0010 and a width (peak-to-peak first derivative) ΔH_{pp} of about 3–5 G. This line can be assigned to the well-known E' center, whose origin is essentially a silicon dangling bond in a $\cdot Si{\equiv}O_3$ configuration.[15,16] This defect was observed in the spectra *a* and *b* of Fig. 7, corresponding to stoichiometric and near-stoichiometric samples, respectively.

(ii) Another wider line (H_{pp} of about 6–9 G) with a g value in the range 2.0045–2.0055. In the literature two defects with similar features are reported: the bulk silicon dangling bond center in $\cdot Si{\equiv}Si_3$ configuration, that some authors call D center[16] and the well-known interface P_b center ($\cdot Si{\equiv}Si_3$ at the SiO_2/Si interface with a g value of 2.005[43]). This defect, which will be called in the following as Si_{DB},

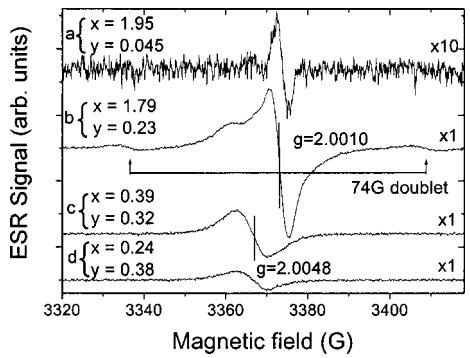

FIG. 7. ESR spectra of four significant as-deposited film compositions: stoichiometric (a), near-stoichiometric (b), and off-stoichiometric (c) and (d).

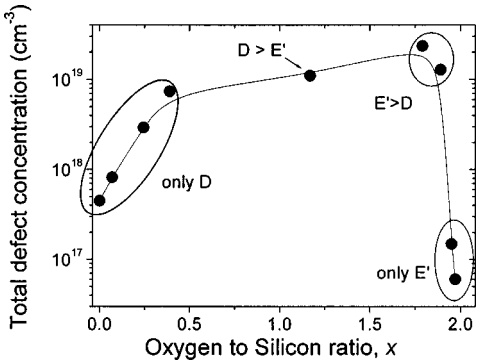

FIG. 8. Total defect concentration of paramagnetically active defects as a function of x. The dominant kinds of defects are depicted by ellipses in the figure. The line is a guide to the eye.

appears in the spectra *b*, *c*, and *d* of Fig. 7, corresponding to near-stoichiometric and off-stoichiometric samples.

(iii) Finally, near stoichiometric samples also exhibit a very weak doublet, separated by 74 G. This is the $E'H$ defect, a dangling bond of a Si atom which is bonded to one H and two O atoms, i.e., in a $\cdot Si{\equiv}O_2H$ configuration.[15]

The type and concentration of each defect were strongly dependent on the film composition,[44] as can be observed in Fig. 7. The total amount of paramagnetic defects as a function of x is depicted in Fig. 8. In this figure the dominant kind of defect is indicated. It was not possible to separate unambiguously the contribution of both types of defects. Figure 8 shows that the dominant kind of defect changed from E' in SiO_2 films to Si_{DB} in off-stoichiometric samples. SiO_2 samples presented a low concentration of defects, around 7×10^{16} cm^{-3} (10^{16} cm^{-3} is the detection limit of this technique). On the other hand, near-stoichiometric samples had the highest defect content of all compositions, with a total defect concentration in excess of 10^{19} cm^{-3}. In these samples a change of the dominant kind of defects undergoes: for $x>1.7$ both E' and Si_{DB} centers were present, but E' centers were dominant. On the other hand, in the samples with $x<1.7$ both centers were also found but the dominant one was the Si_{DB}. For x values below 1.0, only the Si_{DB} defect was detected. On the contrary of what could be expected from the FTIR results (the FWHM of the films indicated that off-stoichiometric films were more disordered), the total defect concentration decreased from the near-stoichiometric value when x decreased.

The 74 G doublet appeared only in samples with $\mathbf{R_b}$ values between 0.3 and 0.55 (stoichiometric/near-stoichiometric limit, see Fig. 8). It was detected only in these samples since these were the only ones containing *H* that had a high E' concentration.

IV. DISCUSSION

A. Stoichiometric films ($x=1.97-1.95$, $y=0.034-0.046$)

These films were deposited with an excess of O_2, which was able to replace most of the hydrogen from the plasma excited SiH_4^* species. Hence, only few H atoms were incorporated into the film, as HI-ERDA measurements showed. Another effect of the high amount of O_2 during the deposition is the absence of Si–Si bonds. If these bonds would exist, the resulting film could not be stoichiometric SiO_2. The indication of the stoichiometry of the film results from the comparison of remaining Si electrons with valence O electrons, from the wave number of the Si–O–Si stretching peak and from the value of the refractive index, which all were consistent with those reported for thermally grown SiO_2. These films presented E' defects in a low amount and when the O_2 content in the plasma decreased $E'H$ defects were also found. The occurrence of E' defects is not surprising since this defect consists of a nonsaturated bond in a $\cdot Si{\equiv}O_3$ configuration. But most silicon bonds are saturated with oxygen (if that would not be the case, the films would not be stoichiometric) and, therefore, this defect type appeared in very low concentrations, and it was the only type detected.

B. Near-stoichiometric samples ($x=1.89-1.79$, $y=0.25-0.23$)

The results obtained from these samples can be explained as follows: the structure of near-stoichiometric films is very similar to the one of stoichiometric SiO_2, as FTIR and ellipsometric results indicate. In stoichiometric SiO_2 each Si atom is bonded to four oxygen atoms. To decrease the overall oxygen to silicon ratio, if an oxygen atom is taken out of the SiO_2 network, two Si atoms are each left with a nonbonded valence electron. These nonsaturated electrons can be saturated by hydrogen creating a $H-Si{\equiv}O_3$ group; a Si–Si bond can be formed; or the electron can remain unbonded creating an E' dangling bond defect. Si–Si bonding should be scarce, because a high amount of these bonds would distort the network (due to differences in bonding distances) giving a higher value of the FWHM in the FTIR spectra. It is also known that the formation of Si–Si bonds is energetically less favorable than the formation of Si–H bonds.[45] Therefore the number of Si–H bonds is significantly higher than in the stoichiometric case. The Si dangling bonds not saturated with hydrogen cause the intense ESR signal. As the formation of a Si–H bond is more favorable than having an unbonded electron,[46] the total amount of bonded hydrogen is about two orders of magnitude higher than the dangling bonds concentration.[33]

In these near-stoichiometric films most Si atoms with a dangling bond are bonded to three oxygen atoms, so the main kind of defect detected was the E' center. As stated before, the Si_{DB} signal can have two sources: P_b centers at the SiO_x/Si interface, and bulk *D* centers. Since the P_b center is a surface defect, it cannot explain the high Si_{DB} content detected for these films. Following the random bonding model (RBM),[47] for these compositions the fraction of Si atoms bonded to three other Si atoms should be marginal, and very few *D* defects should be measured. In our case there is a significant amount of Si_{DB} defects, much higher than what could be expected following the RBM. Inokuma *et al.*[17] found this same discrepancy, which they interpreted as a transfer of electrons between the dangling bond centers

with a different number of oxygen neighbors, were the bulk $\cdot Si{\equiv}Si_3$ configuration is favored (*D* center).

Concerning Si–H bonding, the main Si–H stretching peak appeared at 2260 cm^{-1}. This indicates that most of the hydrogen was bonded in a $H–Si{\equiv}O_3$ configuration, as it was expected from the RBM. The appearance of a shoulder in the low wave number zone of the peak when *x* decreases indicates that the $H–Si{\equiv}(O_2Si)$ and $H–Si{\equiv}(OSi_2)$ groups were also present.

C. Off-stoichiometric films ($x=1.17-0.07$, $y=0.25-0.38$)

In Sec. III it was shown that these samples had a more disordered structure than SiO_2 films, indicated by the high value of the FWHM. This disorder was due to the high Si and H content of the network. These films could not be considered as a rigid SiO_2 network with oxygen vacancies. The high relative content of Si made the network more flexible: Si–Si bonds were favored, as indicated by the intensification of the $H–Si{\equiv}Si_3$ related peaks. The mixture of Si–Si and Si–O bonds made the bonding distance and bond angle more variable along the network, resulting in a high value of the FWHM. The decrease in the total paramagnetic defect concentration when compared to near stoichiometric samples can be explained as follows: if two Si dangling bonds are close, it is very likely that these dangling bonds can interact creating a Si–Si bond. The formation of this bond was possible in these films because the network was less rigid. The high H content is also responsible that most of the Si dangling bonds are saturated with a H atom. This dependence of total paramagnetic defect concentration with *x* was also previously found by Inokuma *et al.*[17]

In off-stoichiometric samples the presence of Si bonded to three other Si atoms is dominant, as predicted by the RBM and confirmed by the position of Si–H related peaks. Thus, the Si_{DB} must be the *D* defect. On the other hand, in these samples the $Si{\equiv}O_3$ group was marginal due to the low O content. This was the reason for the absence of E' centers.

The FTIR spectra showed that the Si–H stretching vibration had its most intense feature at 2060 cm^{-1}. Lucovsky *et al.*[1] proved that the wave number of the Si–H stretching mode depends not only on the first neighbors of the bond but also on the chemical environment, i.e., on the suboxide character of the film. When *x* was above 1.0 the observed wave numbers of all Si–H stretching modes corresponded exactly to those predicted by the model proposed by the NCSU group.[1] But, for oxygen to silicon ratios lower than 1.0 the measured wave numbers of the Si–H stretching modes were significantly higher than the values predicted by this model. The reason for this discrepancy again is the high hydrogen content of our films; the model is based on the effective electronegativity of the second neighbors of the Si–H bond. In the model it is assumed that, as *x* decreases, oxygen atoms (electronegativity equal to 3.44) are substituted by Si atoms (1.9), with a small amount of H (below 10%). In our samples this is not valid, since the H content is well above 20%. Hydrogen has an electronegativity value of 2.2, so the Si–H bond is surrounded by a more electronegative matrix than in the case considered by the NCSU group[1] This higher effective electronegativity of the matrix resulted in a shift of the Si–H stretching peak to higher wave numbers, as observed in the FTIR spectra.

D. $SiH_{0.36}$ film

In these samples the wave number of the $H–Si{\equiv}Si_3$ stretching peak (2060 cm^{-1}) was larger than that reported in the literature for *a*-Si:H films (2000 cm^{-1}). This discrepancy can be explained in the same way as described above for off-stoichiometric films. In the $SiH_{0.36}$ samples, the peak at 795 cm^{-1} does not appear. This peak is generated by a Si–H bond vibrating in the same plane as a Si–O–Si bond. Therefore, since these samples did not have Si–O bonds, this peak was not found.

V. CONCLUSIONS

The structural properties of ECR deposited SiO_xH_y films were studied. The composition of the samples was measured by HI-ERDA and EDX. The structural arrangement of the samples was determined via FTIR. The samples presented compositions between SiO_2 and $SiH_{0.36}$. HI-ERDA and FTIR analysis of the samples also indicated a high amount of bonded hydrogen (more than 10^{22} at cm^{-3} in silicon rich films). A clear correlation between the peaks at 2260 and 890 cm^{-1} has been found, so the correspondence of these peaks to the $H–Si{\equiv}O_3$ stretching and bending vibrations, respectively, has been proved. The four stretching modes of the $H–Si{\equiv}(O_nSi_{3-n})$ group were detected. The most intense ones were the $H–Si{\equiv}O_3$ and $H–Si{\equiv}Si_3$ groups. Intermediate modes were faint and thus hard to resolve. The ellipsometric measurements showed a variation of the refractive index (at $\lambda=632.8$ nm.) from 1.42 to 2.04 when the oxygen to silicon ratio varied from $x=1.2$ to $x=0$. The strong influence of the film composition on its defect structure was confirmed by ESR measurements, which showed a change of the dominant type of paramagnetic defects from E' to *D* as the oxygen to silicon ratio of the samples varied from SiO_2 to off-stoichiometric suboxides.

From the structural characterization it is concluded that stoichiometric samples contain a low amount of defects, and are good quality, almost defect free SiO_2. Near stoichiometric samples show the same network structure as SiO_2, but the oxygen deficiency and the rigidity of the network result in a high amount of dangling bonds. The bonding configuration of off-stoichiometric samples is more disordered than in the near stoichiometric case, but with a lower content of defects. This is justified by the higher flexibility of the network of the off-stoichiometric samples. This flexibility permits the formation of Si–Si bonds (with the annihilation of two dangling bonds), and the high amount of hydrogen also passivates many dangling bond defects.

ACKNOWLEDGMENTS

The authors acknowledge C.A.I. de Implantación Iónica (U.C.M.) for technical support, and especially to Rosa Cimas Cuevas for aid in sample processing, and C.A.I. de Espec-

troscopia (U.C.M.) for providing access to the FTIR spectrometer. This work was partially supported by the Spanish CICYT, under Contract No. TIC 01-1253.

[1] G. Lucovsky, J. Non-Cryst. Solids **227-230**, 1 (1998).
[2] K. T. Queeney, M. K. Weldon, J. P. Chang, Y. J. Chabal, A. B. Gurevich, J. Sapjeta, and R. L. Opila, J. Appl. Phys. **87**, 1322 (2000).
[3] G. B. Alers, D. J. Werder, Y. Chabal, H. C. Lu, E. P. Gusev, E. Garfunkel, T. Gustafsson, and R. S. Urdahl, Appl. Phys. Lett. **73**, 1517 (1998).
[4] F. Irrera and F. Russo, IEEE Trans. Electron Devices **ED-46**, 2315 (1999).
[5] I. Crupi, S. Lombardo, C. Spinella, C. Bongiormo, Y. Liao, C. Gerardi, B. Fazio, M. Vulpio, and S. Privitera, J. Appl. Phys. **89**, 5552 (2001).
[6] D. N. Kouvatsos, V. Ioannou-Sougleridis, and A. G. Nassiopoulou, Appl. Phys. Lett. **82**, 397 (2003).
[7] U. Kahler and H. Hofmeister, Appl. Phys. A: Mater. Sci. Process. **74**, 13 (2002).
[8] D. Nesheva, C. Raptis, A. Perakis, I. Bineva, Z. Aneva, Z. Levi, S. Alexandrova, and H. Hofmeister, J. Appl. Phys. **82**, 4678 (2002).
[9] G. Franzò, A. Irrera, E. C. Moreira, M. Miritello, F. Iacoma, D. Sanfilippo, G. Di Stefano, P. G. Fallica, and F. Priolo, Appl. Phys. A: Mater. Sci. Process. **74**, 1 (2002).
[10] M. L. Green, E. P. Gusev, R. Degraeve, and E. L. Garfunkel, J. Appl. Phys. **90**, 2057 (2001).
[11] S. M. Sze, *Physics of Semiconductor Devices*, (Wiley, New York, 1981).
[12] C. Lin, W. Tseng, M. S. Feng, and B. Lee, J. Appl. Phys. **87**, 2808 (2000).
[13] D. V. Tsu, G. Lucovsky, and B. N. Davidson, Phys. Rev. B **40**, 1795 (1989).
[14] M. Zacharias, D. Dimova-Malinovska, and M. Stutzmann, Philos. Mag. B **73**, 799 (1996).
[15] P. M. Lenahan and J. F. Conley, Jr., J. Vac. Sci. Technol. B **16**, 2134 (1998).
[16] T. Inokuma, L. He, Y. Kurata, and S. Hasegawa, J. Electrochem. Soc. **142**, 2346 (1995).
[17] E. Holzenkampfer, F.-W. Richter, J. Stuke, and U. Voget-Grote, J. Non-Cryst. Solids **32**, 327 (1979).
[18] P. V. Bulkin, P. L. Swart, and B. M. Lacquet, J. Non-Cryst. Solids **226**, 58 (1998).
[19] K. Yoshida, I. Umezu, N. Sakamoto, M. Inada, and A. Sugimura, J. Appl. Phys. **92**, 5936 (2002).
[20] D. Nesheva, I. Bineva, Z. Levi, Z. Aneva, T. Merdzhanova, and J. C. Pivin, Vacuum **68**, 1 (2003).
[21] K. Miyake, S. Kimura, T. Warabisako, H. Sunami, and T. Tokuyama, J. Vac. Sci. Technol. A **2**, 496 (1984).
[22] B. H. Lee, Y. Jeon, K. Zawadzki, W.-J. Qi, and J. Lee, Appl. Phys. Lett. **74**, 3143 (1999).
[23] T. P. Ma, IEEE Trans. Electron Devices **ED-45**, 680 (1998).
[24] M. Losurdo, P. Capezzuto, G. Bruno, G. Perna, and V. Capozzi, Appl. Phys. Lett. **81**, 16 (2002).
[25] P. K. Shufflebotham, D. J. Thomson, and H. C. Card, J. Appl. Phys. **64**, 4398 (1988).
[26] F. L. Martínez, E. San Andrés, A. del Prado, I. Mártil, D. Bravo, and F. J. López, J. Appl. Phys. **90**, 1573 (2001).
[27] F. L. Martinez, A. Del Prado, I. Mártil, G. González-Díaz, W. Bohne, W. Fuhs, J. Rörich, B. Selle, and I. Sieber, Phys. Rev. B **63**, 245320 (2001).
[28] W. Bohne, J. Röhrich, and G. Röschert, Nucl. Instrum. Methods Phys. Res. B **136-138**, 633 (1998).
[29] W. Bohne, S. Hessler, and G. Röschert, Nucl. Instrum. Methods Phys. Res. B **113**, 78 (1996).
[30] W. Bohne, W. Fuhs, J. Röhrich, B. Selle, I. Sieber, A. del Prado, E. San Andrés, I. Mártil, and G. González-Díaz, Surf. Interface Anal. **34**, 749 (2002).
[31] G. F. Bastin and H. J. M. Heijligers, Scanning **12**, 225 (1990).
[32] B. J. Hinds, F. Wang, D. M. Wolfe, C. L. Hinkle, and G. Lucovsky, J. Vac. Sci. Technol. B **16**, 2171 (1998).
[33] E. San Andrés, A. del Prado, I. Mártil, G. González-Díaz, D. Bravo, and F. J. López, J. Appl. Phys. **92**, 1906 (2002).
[34] F. Rochet, G. Dufour, H. Roulet, B. Pelloie, J. Perrière, E. Fogarassy, A. Slaoui, and M. Froment, Phys. Rev. B **37**, 6468 (1988).
[35] A. Sasella, A. Borghesi, F. Corni, A. Monelli, G. Ottaviani, R. Tonini, B. Pivac, M. Bachetta, and L. Zanotti, J. Vac. Sci. Technol. A **15**, 377 (1997).
[36] D. Landheer, Y. Tao, J. E. Hulse, T. Quance, and D.-X. Xu, J. Electrochem. Soc. **143**, 1681 (1996).
[37] E. San Andrés, A. del Prado, F. L. Martínez, I. Mártil, D. Bravo, and F. J. López, J. Appl. Phys. **87**, 1187 (2000).
[38] K. Furukawa, Y. Liu, H. Nakashima, D. Gao, K. Uchino, K. Muraoka, and H. Tsuzuki, Appl. Phys. Lett. **72**, 725 (1998).
[39] L. He, Y. Kurata, T. Inokuma, and S. Hasegawa, Appl. Phys. Lett. **63**, 162 (1993).
[40] G. Lucovsky, J. Yang, S. S. Chao, J. E. Tyler, and W. Czubatyj, Phys. Rev. B **28**, 3225 (1983).
[41] G. Lucovsky and W. B. Pollard, J. Vac. Sci. Technol. A **1**, 313 (1983).
[42] *Handbook of Optical Constants of Solids*, edited by E. D. Palik (Academic, Orlando, FL, 1985).
[43] M. J. Uren, J. H. Stathis, and E. Cartier, J. Appl. Phys. **80**, 3915 (1996).
[44] E. San Andrés, A. del Prado, I. Mártil, G. González-Díaz, F. L. Martínez, D. Bravo, and F. J. López, Vacuum **67**, 531 (2002).
[45] L. He, T. Inokuma, and S. Hasegawa, Jpn. J. Appl. Phys., Part 1 **35**, 1503 (1996).
[46] H. Angermann, W. Henrion, and A. Röseler, *Silicon-Based Materials and Devices*, Vol. 1: *Materials and Processing* (Academic, New York, 2001) Chap. 7, p. 267.
[47] H. R. Philipp, J. Phys. Chem. Solids **32**, 1935 (1971).